

1 Supplement of
2 **Secondary organic aerosol production from pinanediol, a semi-**
3 **volatile surrogate for first-generation oxidation products of**
4 **monoterpenes**

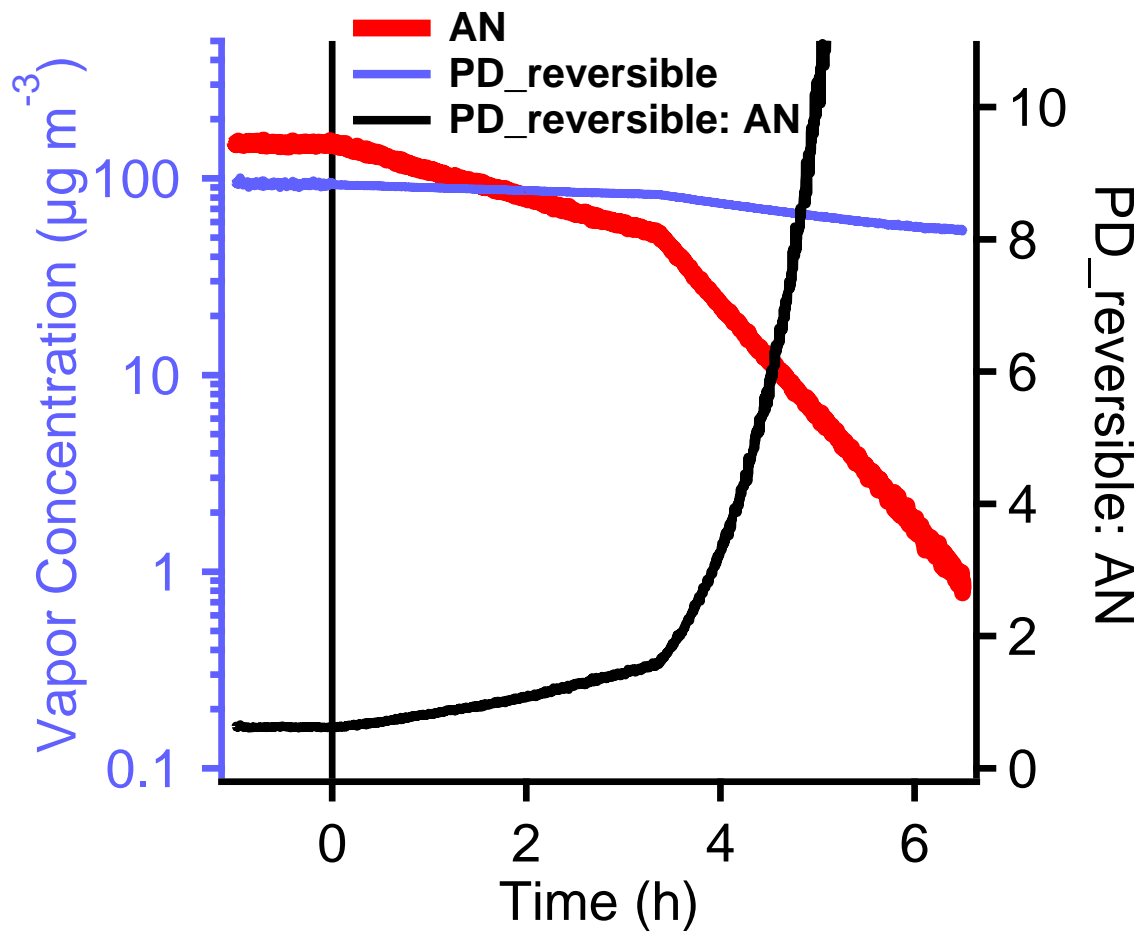
5 Penglin Ye^a, Yunliang Zhao, Wayne K. Chuang, Allen L. Robinson, Neil M. Donahue*

6 Center for Atmospheric Particle Studies, Carnegie Mellon University, 5000 Forbes Avenue, Pittsburgh,
7 Pennsylvania 15213, United States

8 ^anow at: Aerodyne Research Inc, Billerica, MA 01821, USA

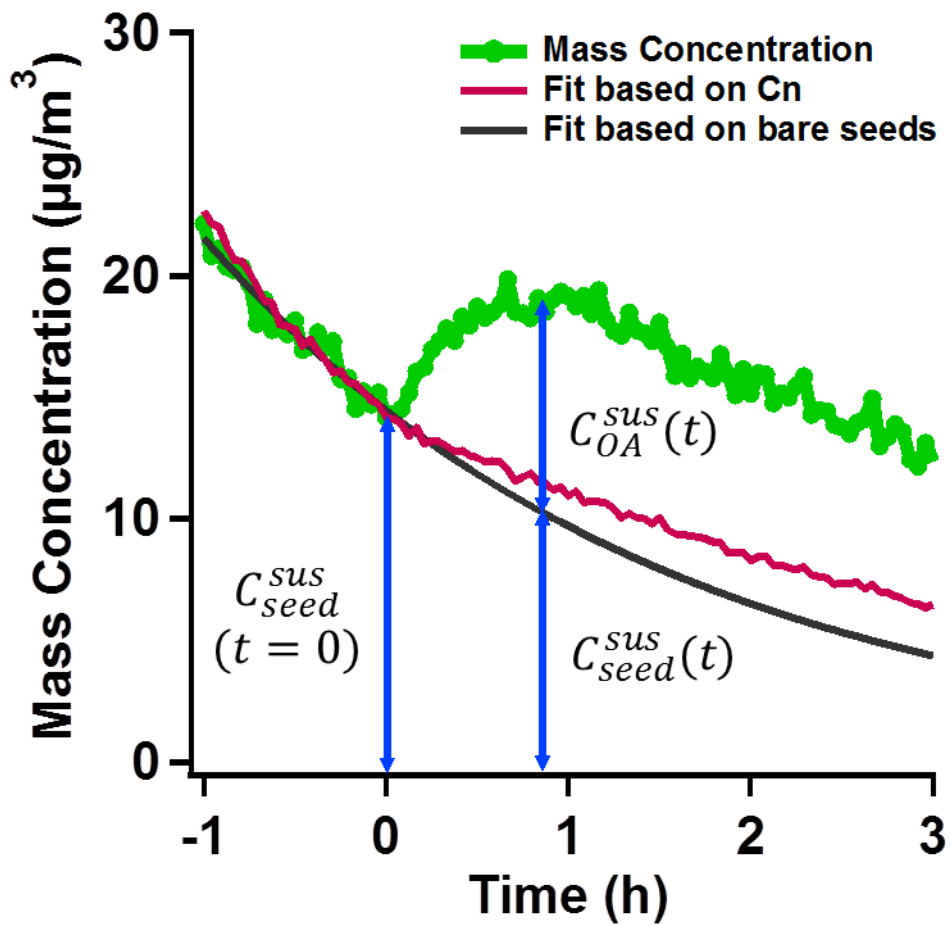
9
10
11
12
13
14
15
16 **Correspondence to: nmd@andrew.cmu.edu*

17
18 Phone: (412) 268-4415



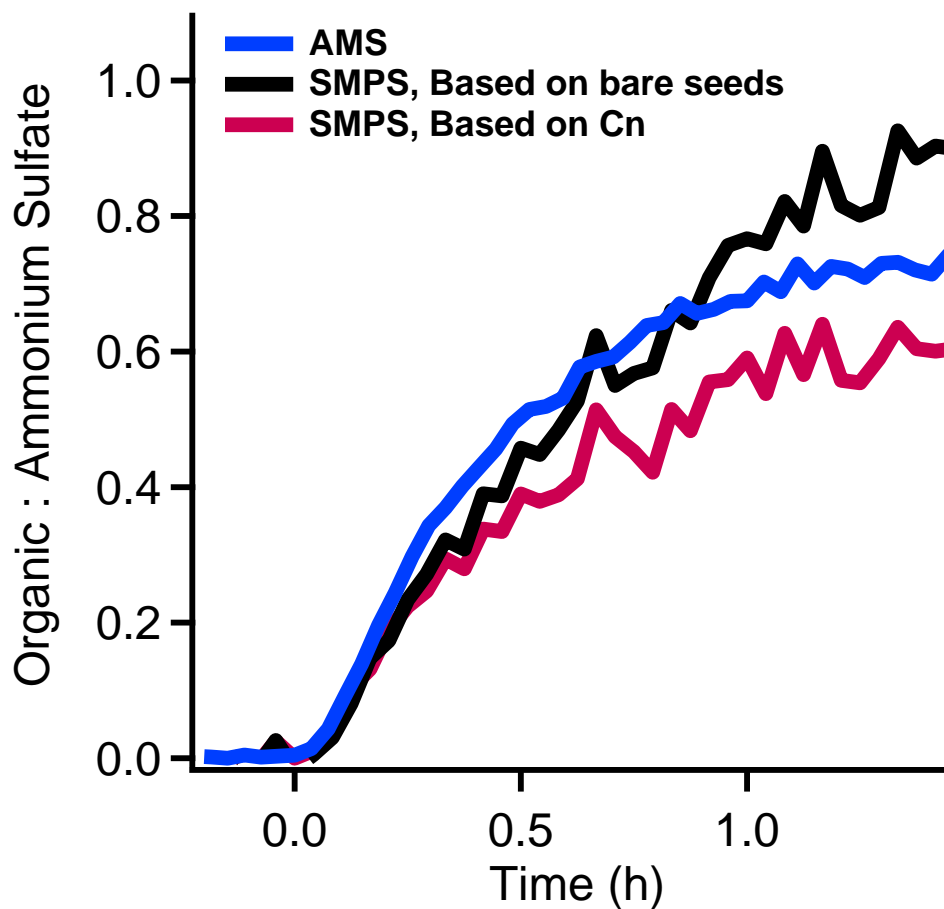
19

20 Figure S1. The predicted PD concentration change during the dilution when considering the deposition of PD on the
 21 Teflon chamber walls as reversible partitioning. The decrease of the predicted PD concentration should be slower
 22 than the decrease of AN. The ratio of the predicted PD to AN concentration should keep increasing.



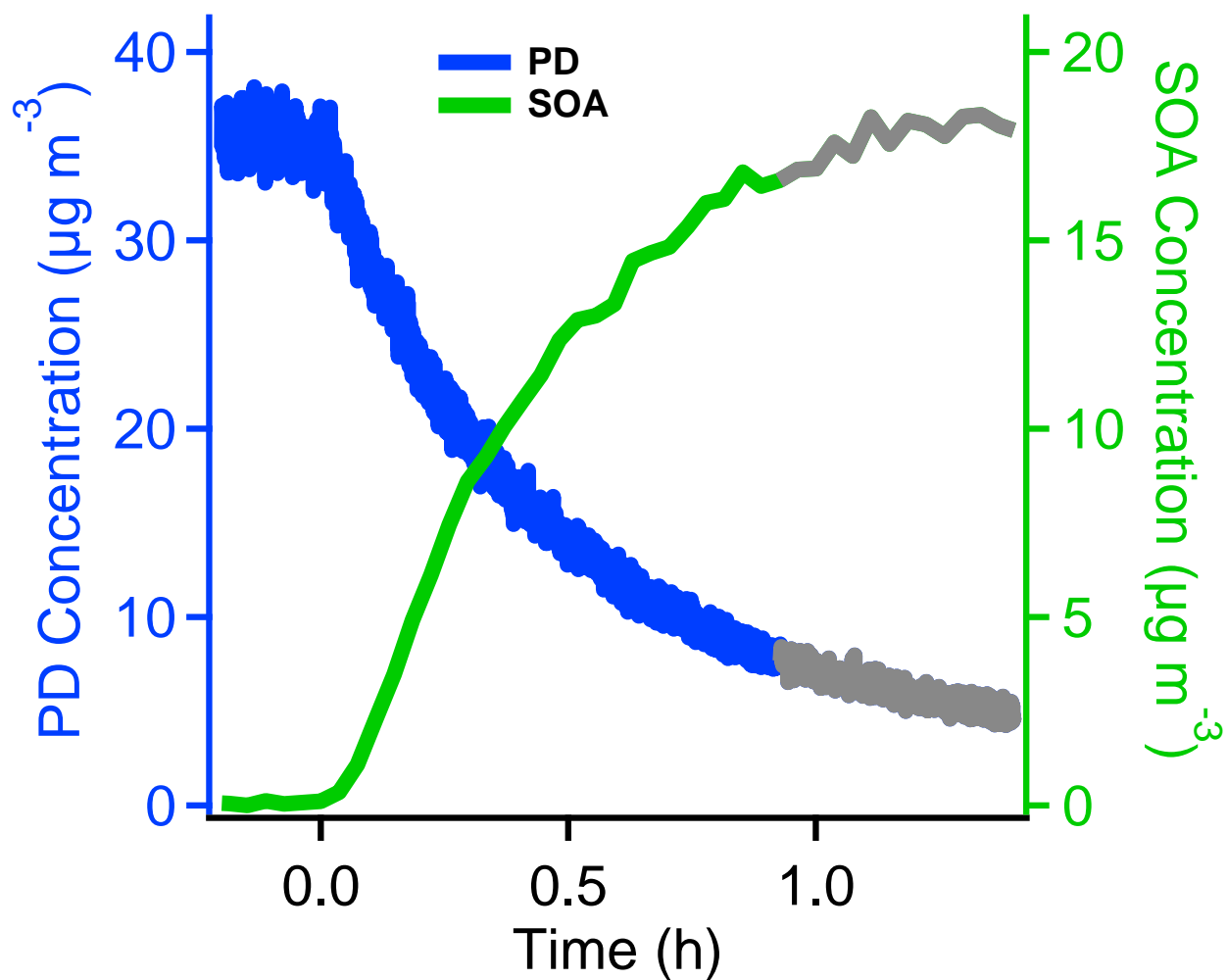
23

24 Figure S2. The particle wall loss correction using method 2 and 3. In method 2, $C_{seed}^{sus}(t)$ was determined by
 25 applying an exponential function to fit the decay of the pure ammonium sulfate seeds and extrapolate it to the whole
 26 experiments (black). $C_{seed}^{sus}(t)$ was also calculated by scaling the total particle number concentration, C_n with the
 27 average particle mass in method 3 (red). $C_{SOA}^{sus}(t)$ is the difference between the total particle mass concentration with
 28 the $C_{seed}^{sus}(t)$. $C_{seed}^{sus}(t)$ and $C_{SOA}^{sus}(t)$ were both corrected with their densities, 1.78 and 1.4 g cm⁻³, respectively.



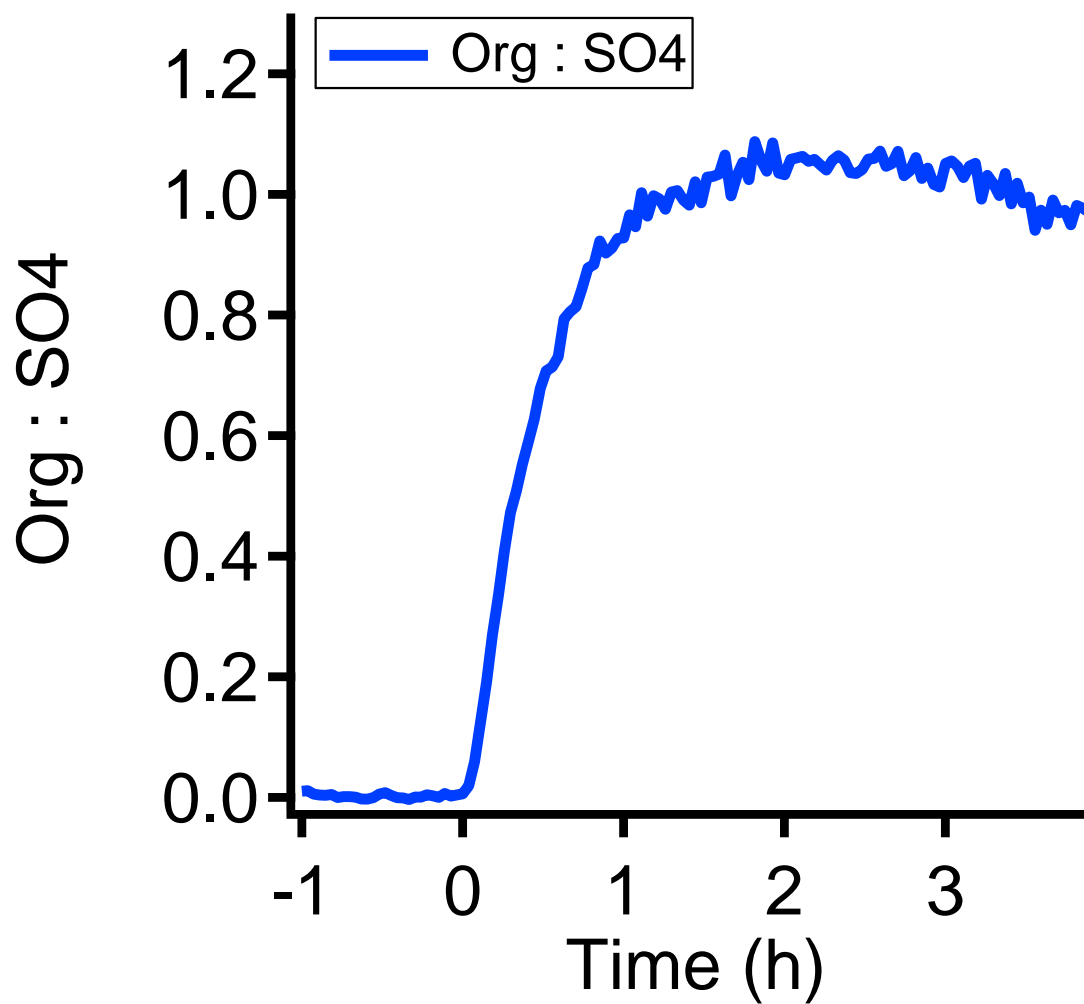
29

30 Figure S3. The ratio of organic to ammonium sulfate seed calculated from three methods, directly from AMS
 31 measurement in Method 1 (blue), determining the ammonium sulfate seed mass by fitting the decay of the pure
 32 seeds and extrapolating it to the whole experiments in Method 2 (black), or by scaling the total particle number
 33 concentration, C_n by the average particle mass in method 3 (red). The ratios from all three methods match well with
 34 each other. So we only focused on the HR-AMS data to do the particle wall loss correction.



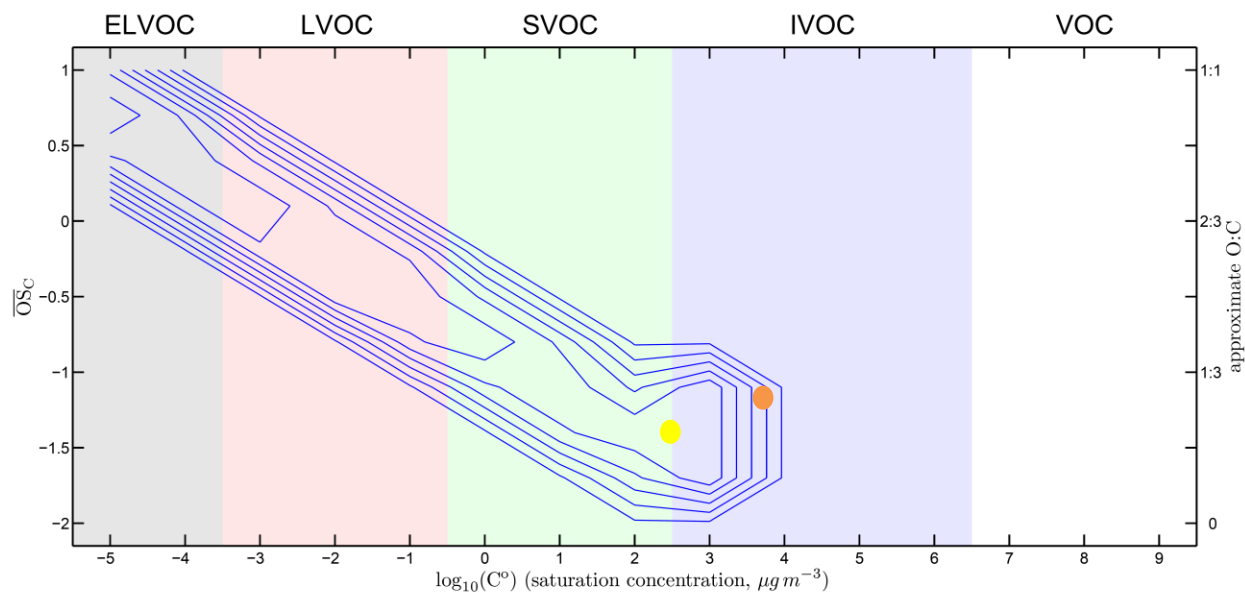
35

36 **Figure S4.** The temporal depletion of PD and formation of SOA. Around 80% of PD were reacted in the first hour.
 37 The gray part (less than 22% of its initial value) was not used when calculating the SOA mass yields.

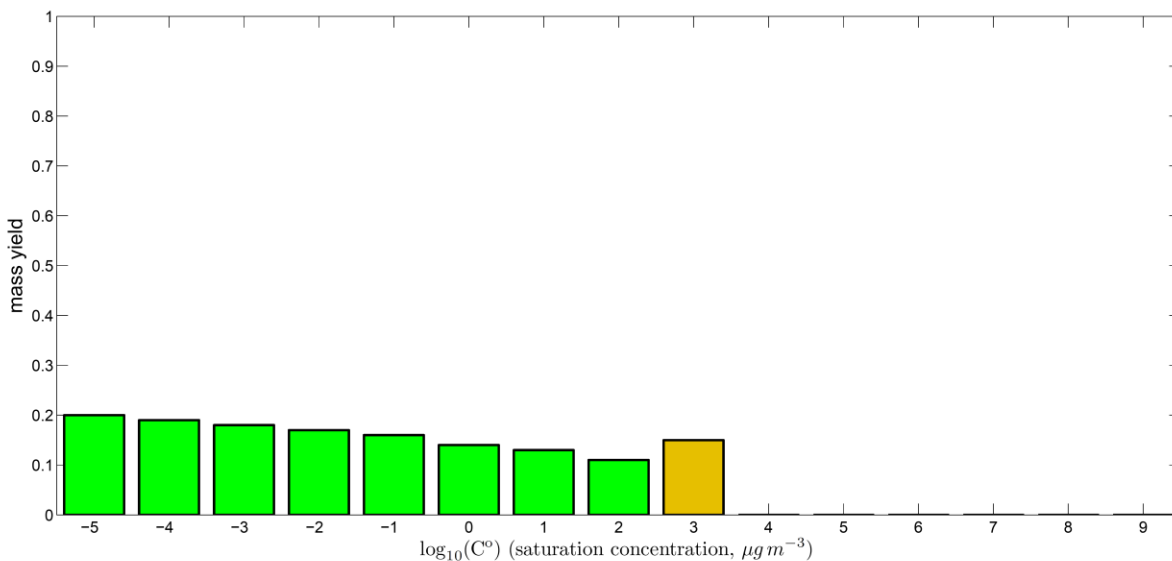


38

39 **Figure S5.** The change of the ratio of organic to sulfate mass from HRAMS measurement. The slight decrease after
40 2 hours indicated the mass loss from the particles. This may be due to the vapor wall loss which triggers the
41 evaporation of the organics on the particles.

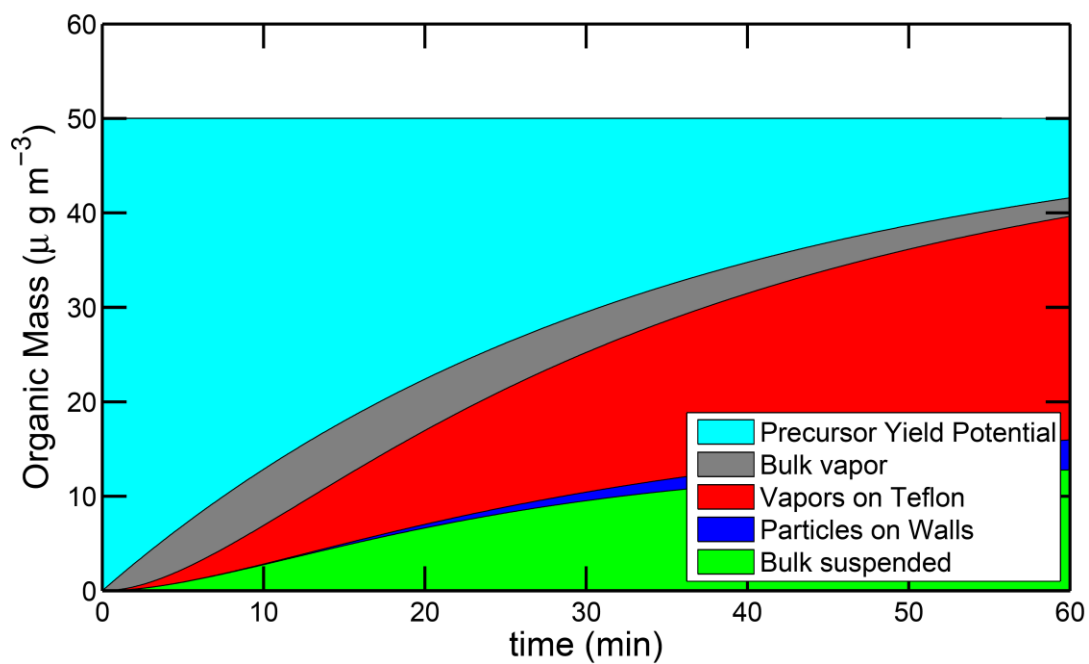


42



43

44 **Figure S6.** Representation of the oxidation products from PD in the two-dimensional volatility-oxidation space
 45 when mass accommodation α equals to 0.1. We group organics in the broad classes of ELVOCs, LVOCs, SVOCs or
 46 IVOCs. The top panel is a 2D representation. PD is shown as a yellow dot. The blue contours show the oxidation
 47 product contours, with higher values indicating higher yields. The lower panel is a 1D consolidation of the 2D
 48 product contours, showing the total mass yields. The major products move to the top left and show more oxidized
 49 and less volatile. In this case, ELVOC and LVOC contribute to around 60% of total aerosol mass. ELVOCs and
 50 LVOCs usually have very high or unit mass accommodation coefficient, which contradict to the assumption, α
 51 equals to 0.1. So α equals to 0.1 may not be the proper value for the SOA studied here.



52

53 **Figure S7.** Dynamical simulation of the SOA production from 6ppb PD with mass accommodation coefficient $\alpha=0.1$.
 54 The simulation treats five different reservoirs: unreacted precursor, vapors, suspended particles, deposited particles,
 55 and sorption to teflon, as shown in the legend.